Influence of the flow field in curtain coating onto a prewet substrate

J. O. Marston and M. J. H. Simmons
Department of Chemical Engineering, University of Birmingham, Edgbaston, Birmingham B15 2TT, United Kingdom

S. P. Decent and S. P. Kirk
School of Mathematics, University of Birmingham, Edgbaston, Birmingham B15 2TT, United Kingdom

(Received 21 July 2006; accepted 29 September 2006; published online 9 November 2006)

The onset of air entrainment for curtain coating onto a surface prewetted with the coating fluid was studied. The substrate used was a polished, scraped steel wheel and coating was performed over ranges of dimensionless parameters observed in commercial coating processes (Reynolds number, $0.14<\mathrm{Re}=\rho Q/\mu<33.02$; Capillary number, $0.19<\mathrm{Ca}=\mu U/\sigma<25.07$). The substrate velocity for the onset of air entrainment was obtained as a function of the curtain flow rate per unit width of curtain ($1<Q<9$ cm^2 s^{-1}), fluid dynamic viscosity ($0.0326<\mu<0.878$ Pa s), curtain height ($0.035<h<0.095$ m), and thickness of the prewet film ($1\times10^{-7}<c<3\times10^{-5}$ m). A remarkable and strong dependence of the onset of air entrainment on curtain flow rate was observed (hydrodynamic assist) and the general features of the hydrodynamics were very similar to those observed for previous works onto dry substrates. However, the presence of the prewet film led to higher maximum substrate velocities at the onset of air entrainment than observed for dry substrates. For high liquid viscosities, the air entrainment curve bifurcates; under these conditions, the maximum substrate velocity is no longer inversely proportional to the fluid viscosity and stable coating is possible at higher substrate velocities than would be predicted by conventional theory. This "intense assist" exhibits a complex relationship with the prewet film thickness. The results presented in this paper demonstrate that hydrodynamic assist is not exclusive to wetting, but is a generic phenomenon of fluid flows. © *2006 American Institute of Physics*.
[DOI: 10.1063/1.2378562]

I. INTRODUCTION

The use of thin films of liquid to coat solid substrates is a highly important process for the production of photographic film and paper, specialist papers for use in inkjet printing, and for the creation of protective layers on reactive solid surfaces. A key driver for industries employing these techniques is the need to produce defect-free coatings as rapidly as possible, hence the speed of operation of the coating process needs to be maximized.

In the conventional curtain coating process, a falling thin liquid sheet impinges upon a moving solid substrate; this forms a three-phase wetting line where the liquid film displaces air at the solid surface, creating a dynamic contact angle (θ_d) between the free surface of the liquid and the solid substrate. This dynamic wetting process remains a great unsolved problem in fluid mechanics since the inclusion of the contact line in the classical hydrodynamic model leads to a shear-stress singularity.[1] The choice of physical models (e.g., molecular-kinetic, hydrodynamic, or some combination) for the shape and behavior of the free surface in the vicinity of the contact line is still the subject of considerable debate (see Blake[2] for an authoritative review).

Conventional fluid mechanics suggests that the dynamic contact angle should be a function only of the contact line speed and the material and fluid properties for any given coating process. For example in dip coating, for smooth substrates, the dynamic contact angle can be correlated in terms of a Capillary number ($\mathrm{Ca}=\mu U/\sigma$, where U is the substrate velocity, μ is the dynamic viscosity, and σ is the surface tension).

However, Blake *et al.*[3,4] showed that in curtain coating, the global hydrodynamics and geometry of the flow had a powerful influence on the onset of air entrainment and the dynamic contact angle in curtain coating. This led to the possibility of wetting speeds several orders of magnitude higher than is possible for dip coating via the alteration of parameters affecting the flow field, e.g., the curtain height h and the liquid flow rate Q; this effect was termed *hydrodynamic assist*. This phenomenon was recently observed for the dynamic contact angle evolution in impacting drops by Šikalo *et al.*[5]

At speeds above a maximum substrate velocity, dynamic wetting failure will occur, which in industrial coating processes is characterized by the entrainment of air bubbles at the wetting (contact) line, creating defects in the coated film layer. Air entrainment occurs when the dynamic contact angle exceeds $\theta_{\max}$ ($<180°$), which is dependent on the gas-liquid-solid system of interest. This phenomenon has been observed in several film coating processes, e.g., dip coating,[6–8] roll coating,[9,10] and curtain coating.[3,4,11,12]

Many empirical relationships for the onset of air entrainment exist,[8] for example the equation of Burley and Jolly,[13]

$$U_{ae} = 0.395\left(\frac{\sigma}{\mu}\right)^{0.77} \quad (1)$$

with μ in mPa s and σ in mNm^{-1}.

Methods of promoting wetting to higher speeds and hence postponing air entrainment without changing the flow field include angling of the wetting line,[14] use of roughened substrates,[8,11,15] the use of electric fields,[16] prewetting the solid surface,[17,18] or the inclusion of a low-viscosity carrier layer in the main fluid deposit.[19,20]

It is surprising that no comprehensive studies exist in the open literature of the effect of prewetting the solid surface in coating operations, given the profound effect this is likely to have on the maximum speed of wetting. For example, Yamamura *et al.*[21] demonstrated hydrodynamic assist in the onset of air entrainment for a liquid jet impinging onto a scraped wheel, yet did not consider the influence of the residual fluid carryover as a parameter in their analysis. Chen *et al.*[17] demonstrated for a dip-coating arrangement that viscous bending of the free surface approaching the substrate was broadly dependent upon whether the thickness of the prewetted layer was "thin," i.e., of $O(10^{-9}-10^{-8})$ m, or "thick" of $O(10^{-6})$ m.

When the solid surface is prewetted, the coated film is incorporated into the existing fluid layer on the surface. As such, air entrainment must occur between two liquid interfaces of the same properties, hence the flow close to the contact line (where the impinging film in the curtain meets the pre-existing layer) may be considered similar to that observed by Joseph *et al.*[22] for the formation of a two-dimensional free-surface cusp, produced by counter-rotating cylinders partly immersed in fluid. In this experimental study, the observed shape of the free surface passed through a transition from a rounded interface with a stagnation point to a cusped interface with a singularity of curvature, at the resolution of the experiments. For Newtonian fluids, this process was shown to be smooth and gradual, eventually leading to the development of a cusp, while for non-Newtonian fluids the transition was sudden. In a related study, Lorenceau *et al.*[23] showed that the onset of air entrainment could occur before the onset of cusping; this was explained by Eggers[24] as due to the lubrication pressure of the air drawn into the cusp. This situation is analogous to the onset of dynamic wetting failure where air entrainment can occur before the dynamic contact angle reaches 180°. Other analogies between cusp formation and dynamic wetting were made by Joseph.[25] The analogy made here is simply to underline the fact that, for a prewetted surface, air entrainment must occur between two liquid interfaces and is not based on observation, nor is it to understand the nature of or existence of cusps; this has received significant attention since the work of Joseph (see, e.g., Refs. 24 and 26–28).

This paper describes a series of experiments using a pilot-scale curtain coating facility to determine how the onset of air entrainment and profile of the free surface is influenced by the global flow field and fluid properties in the presence of a thin film prewetting the solid substrate. Aqueous solutions of glycerol with viscosities ranging from $0.0326 < \mu < 0.878$ Pa s were used and the influence of curtain flow rate, Q, curtain height, h, and film thickness, c, were studied. The results provide the first observations of the mechanism of hydrodynamic assist in a curtain geometry onto a prewet surface, thus showing that hydrodynamic assist, i.e., the manipulation of the flow to postpone air entrainment, is not exclusive to dynamic wetting.

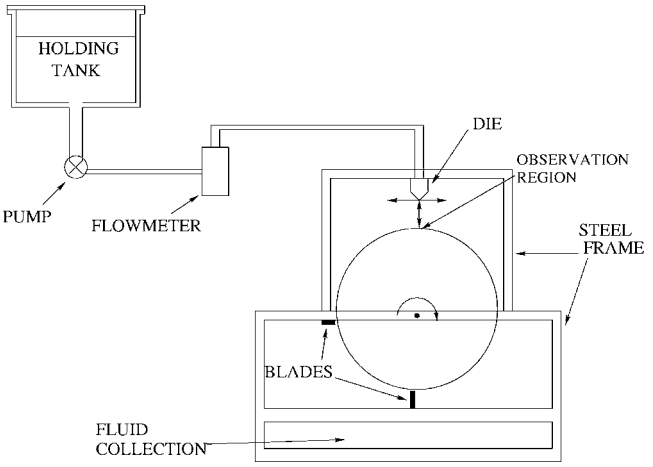

FIG. 1. Experimental apparatus.

II. MATERIALS AND METHODS

A schematic of the pilot-scale curtain coating facility is shown in Fig. 1. The continuous substrate was provided by a rotating stainless steel wheel, with a diameter of 0.45 m and a width of 0.06 m. The surface was highly polished so that the average surface deviation was 52±2 nm as measured by an atomic force microscope (AFM). The wheel was driven by a 0.55 kW motor with inverter feedback control (Eurotherm 690+ series) producing a range of substrate velocities from 0.15–2.3 ms^{-1}.

The fluids used were aqueous solutions of glycerol (Croda, UK) and the properties for the fluids used at the temperature of the experiments are given in Table I. The fluid dynamic viscosities were measured using a Contraves Rheomat-30 viscometer equipped with a cup and bob attach-

TABLE I. Properties of glycerol-water mixtures at laboratory temperature of experiments (approximate concentrations by weight).

Fluid	Viscosity (Pa s)	Density (kgm^{-3})	Surface tension (Nm^{-1})
72% glycerol soln	0.0326	1196	0.0678
75% glycerol soln	0.041	1208	0.0664
82% glycerol soln	0.0839	1235	0.0672
85% glycerol soln	0.124	1241	0.0664
90% glycerol soln	0.245	1253	0.0655
94% glycerol soln	0.365	1262	0.065
95% glycerol soln	0.427	1264	0.0647
95.5% glycerol soln	0.462	1265	0.065
96% glycerol soln	0.552	1266	0.0648
97% glycerol soln	0.706	1269	0.0647
98% glycerol soln	0.878	1270	0.0642

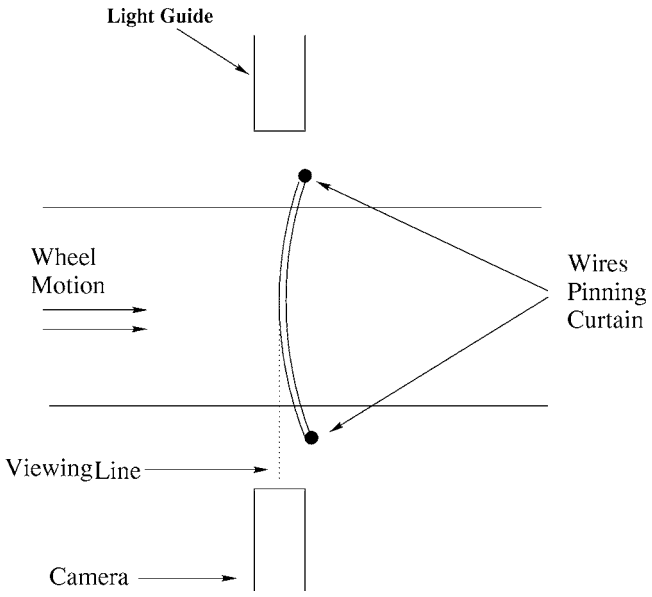

FIG. 2. Plan view of the impingement of the curtain.

ment. Surface tensions were measured using a du Nouy ring tensiometer. Measurements of these properties were made over a range of temperatures enabling the correct values to be used given the temperature of the fluids used within the facility. Due to ambient laboratory conditions, fluid temperatures varied from 19–24 °C, however the temperature of the fluids used remained constant over the duration of a single experiment.

The fluids were supplied to a four-slot die of width 0.09 m (based on a design by Kodak Ltd., UK) using a high accuracy gear pump (Series 200, Liquiflo, USA). Flow rates, measured by an electromagnetic flow meter (IFM5020K/D, Krohne, Germany), ranging from $1-10\ \mathrm{cm^2\ s^{-1}}$ (defined per unit width of curtain) were possible. The flow meter was calibrated by weighing collected fluid over certain time intervals and flow rates and was determined to be accurate to within 3.5%. The integrity of the falling curtain was maintained by using copper wires of 1.6 mm diameter as edge guides (for low viscosity fluids) and perspex windows (for high viscosity fluids).

Visualization of the free surface at the wetting line was achieved for low viscosity fluids by bending the edge guides forward out of the plane of the curtain, to allow a clear and undistorted view of the wetting line at the center of the curtain through the ambient air, as shown in Fig. 2. The influence of this curvature on the central region of the curtain was negligible. Images were obtained using a traveling microscope with a maximum possible optical resolution on the order of micrometers (based on the diffraction limit of the lens) depending on the magnification used, although since several pixels were needed to determine the location of the contact point, the maximum resolution could only be claimed conservatively at an order of magnitude higher than this value, i.e., $O(10\ \mu\mathrm{m})$. As such, it was chosen not to study the dynamic contact angle, but rather image the free-surface profile as a whole. A 1280×1024 pixel CCD camera (7800 series, Cohu Inc., USA) and image grabber attached to a personal computer was used to capture the images. Back illumination was provided by a 90 W fiber optic light guide placed behind the rear of the curtain. To study the free-surface shape close to the contact line, a higher magnification was used in combination with a high-speed camera (Fastcam Super 10 K Series Model 3000, Photron Ltd., UK) with a recording speed between 250 and 10 000 frames per second.

Removal of the bulk of the liquid film from the solid substrate after coating was performed using a series of urethane double-v "squeegee" blades (Perforag Ltd., UK). By changing the tension of the blades, the amount of the residual film remaining on the wheel could be altered. Estimates of the thickness of the film were produced by placing absorbent material onto the rotating wheel before the coating die for 10 revolutions during the coating process. The film thicknesses were deduced from the weight of fluid absorbed. Results indicate that the film thickness is consistently of the order of 10^{-6} m (unless otherwise stated). These then fall into the classification of "thick," as described by Chen *et al.*[17] The precise thickness of the residual film could not be preset at a specific value using this method, however repeatability of both the onset velocities and the thicknesses of the film at various points in the parameter space of interest indicate that the thickness is independent of curtain flow rate and does not vary dynamically throughout the course of any experiments, i.e., c is not a dynamic variable. This is discussed in detail later.

Measurements of the wheel velocity at the onset of air entrainment were made for each of the fluids given in Table I at set curtain heights of 35, 65, 85, and 95 mm. The onset of air entrainment was obtained by increasing the substrate (wheel) velocity at constant curtain flow rate, Q, until wetting (coating) failure and entrainment of air bubbles was observed with the naked eye. In true dynamic wetting problems, dynamic wetting failure—where the wetting line ceases to advance normal to itself and adopts a sawtooth configuration—can occur before the onset of air entrainment. Equally, when the surface is prewetted, the liquid may fail to coat the surface before air entrainment occurs, however these two points could not be distinguished in these experiments, as also observed by Cohu and Benkreira[29] for dip coating.

To repeat measurements, the substrate velocity was decreased from the onset of air entrainment until clearance, where no bubbles were seen and stable coating resumed. There was a notable difference between the velocities at the onset and clearance of air entrainment in all cases, which produces regions of hysteresis. This phenomenon is addressed in more detail by Marston *et al.*,[30] however all data presented here are for the onset of air entrainment obtained by increasing the substrate velocity for fixed curtain flow rates.

The procedure was then repeated for higher values of curtain flow rate, Q, until the substrate velocity at the onset of air entrainment was no longer a function of Q. Each data point was repeated a minimum of three times and the observed variation was less than 3%.

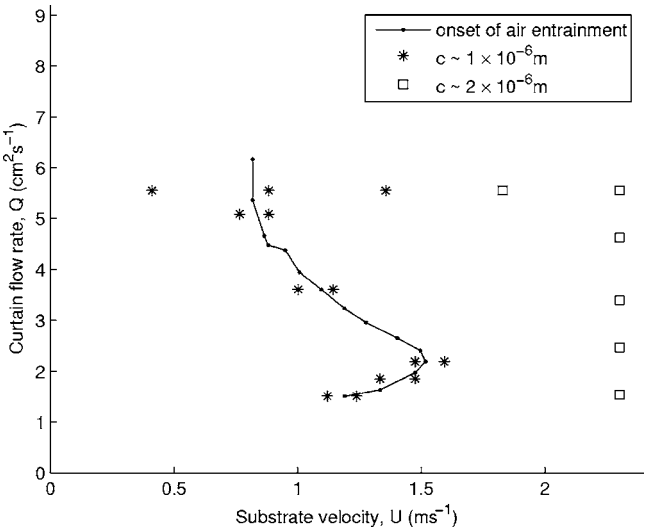

FIG. 3. Air entrainment onset curve for a 0.07 Pa s solution (ρ=1228 kgm^{-3}, σ=0.0671 Nm^{-1}) with a curtain height of 60 mm. The plot also marks locations throughout the $Q-U$ parameter space at which residual film thicknesses were measured. The estimates, based on volume of fluid absorbed through 10 revolutions, identify that the thickness, c, is very weakly dependent upon U, but independent of Q.

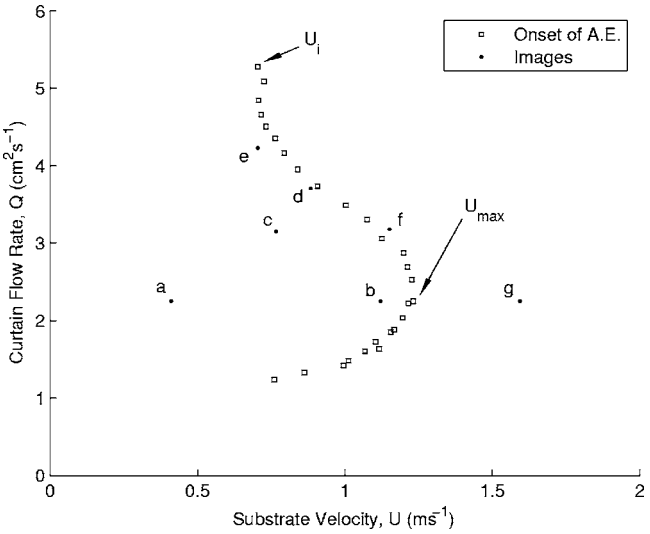

FIG. 4. Air entrainment onset curve for 0.0839 Pa s solution with curtain height of 65 mm, with the location of images of the free surface, as given in Fig. 5. $c \sim 10^{-6}$ m.

III. RESULTS AND DISCUSSION

Figure 3 shows the substrate velocity, U, at the onset of air entrainment plotted as a function of the curtain flow rate, Q, for a 0.07 Pa s glycerol solution. A clear dependence of U upon the flow field is shown; U reaches a maximum value, U_{max}=1.52 ms^{-1} at Q=2.19 cm^2 s^{-1}. At high values of Q, the value of U becomes independent of the flow field, U_i. The remarkable result is that the shape of the curve is typical for air entrainment data using the curtain coating method onto a dry substrate.[3,4,31] Figure 3 also indicates points throughout the $Q-U$ plane at which measurements of the film thickness, c, were made. These were ~1 or 2 μm depending on the wheel speed. The measurements show that the film thickness is independent of Q and only weakly dependent on U. Hence, over the ranges of Q and U defining the air entrainment curve, c may be taken as constant. Calculations were performed for other viscosities tested and similar trends were noted. All measurements show that $c \sim O(10^{-6})$ m.

Figure 4 shows a similar air entrainment curve for a 0.0839 Pa s coating fluid. In this case, U_{max}=1.25 ms^{-1} at Q=2.25 cm^2 s^{-1}. The points marked (a–g) on the air entrainment curve correspond to the locations of the free surface profiles at the back of the curtain shown in Fig. 5. All of the locations marked to the left of the air entrainment curve (a–e) represent successful coating. In Fig. 5(e), where the wetting line is considerably upstream of the falling curtain, the wetting line becomes isolated from the effects of the curtain flow field. Figures 5(f) and 5(g) illustrate images taken when air entrainment was indeed occurring, although this is not immediately obvious from these images. They also show that air entrainment can occur with or without the formation of a heel; in Fig. 5(f), the large heel is due to the reduction in viscous drag caused by the entrained air film. Using a high-speed camera (at 6.75× magnification) allows more detail of the free surface at the contact line to be resolved. The representative images presented in Fig. 6 are taken for a 0.041 Pa s coating fluid at a constant curtain flow rate of Q=3.21 cm^2 s^{-1} and curtain height h=60 mm. Images (a) and (b) are taken for substrate velocities of 0.24 and 0.41 ms^{-1}, respectively. Figure 6(a) shows the rear section of a large heel formation; the image shows rapid changes in curvature of the rear free surface of the impinging liquid on the scale of 20–30 μm.

This phenomenon is also apparent from the image at higher speed; Fig. 6(b) shows a reduced heel (due to increased substrate velocity) and a small degree of viscous bending of the free-surface close to the contact line; further increases in substrate speed sharpen the interface [e.g., Fig. 5(f)] until the air drawn in between the two liquid interfaces can no longer be suppressed and is eventually entrained into the coated film. Both Figs. 6(a) and 6(b) were taken well within the stable coating window, supported by the fact that the apparent dynamic contact angles are $\leqslant 90^{\circ}$.

Figures 7(a)–7(c) show air entrainment data, plotted as curtain flow rate versus substrate velocity for curtain heights of 35, 65, and 85 mm, respectively. As shown in Figs. 3 and 4, a strong dependence of the substrate velocity at air entrainment on the curtain flow rate, i.e., hydrodynamic assist, is observed at all curtain heights and fluid viscosities tested. At low curtain flow rates, Fig. 7(a) shows large increases in U for marginal increases in Q for the 0.0326 and 0.0839 Pa s solutions, and the maximum substrate velocity is observed at a lower curtain flow rate than observed for the higher viscosity solutions. The higher viscosity solutions do not appear to exhibit as high a dependence on the curtain flow rate as the low viscosity solutions and, at high curtain flow rates, appear to be approaching a similar substrate velocity. The maximum substrate velocity obtained decreases with increasing viscosity. The data shown in Figs. 7(b) and 7(c) for 65 and 85 mm curtain heights exhibit similar trends.

The data for all of the viscosities presented in Fig. 7

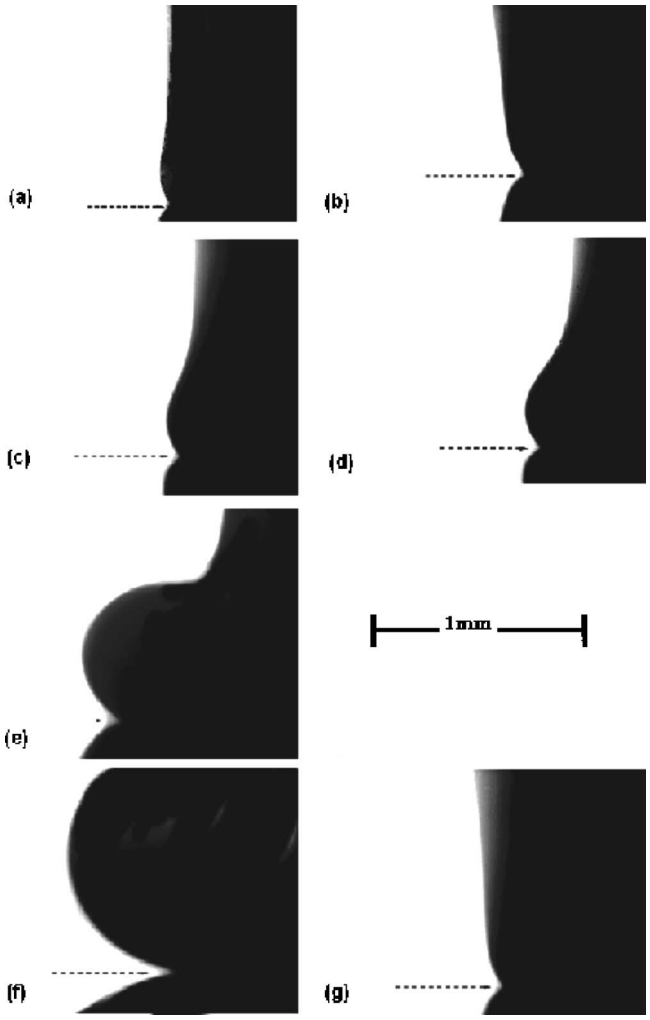

FIG. 5. Free surface profiles for the 0.0839 Pa s solution. The images correspond to those located on the air entrainment graph in Fig. 4. A reference length scale has been included. The dashed line represents the wheel surface.

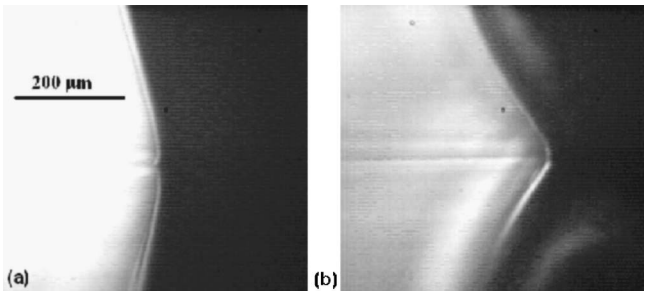

FIG. 6. Images in the vicinity of the contact line for a 0.041 Pa s solution. Images are for a constant curtain flow rate $Q=3.21\ \mathrm{cm^2\ s^{-1}}$ and height $h=60$ mm. For image (a), $U=0.24\ \mathrm{ms^{-1}}$. For image (b), $U=0.41\ \mathrm{ms^{-1}}$. Images are taken at 6.75× magnification with the high speed camera giving a resolution of $\sim 10\ \mu$m. $c\sim 10^{-6}$ m. A reference length scale is included.

could be examined for increasing curtain height. It was chosen not to replot the data, but analysis shows, for example, that for the 0.0326 Pa s solution, increasing the height from 35 to 85 mm leads to an increase of the maximum substrate velocity ($U_{\max}$) from 1.25 to 1.66 $\mathrm{ms^{-1}}$. Similar increases are noted for all fluid viscosities. A feature common for all the low fluid viscosities used is that higher substrate velocities are attainable at lower curtain heights for flow rates above the maximum substrate velocity.

Data from Figs. 3, 4, and 7 show that U approaches a limiting value at high curtain flow rates where there is no further dependence of the contact line behavior upon the hydrodynamics of the flow field. Once this point is reached, the dominant forces acting at the contact line are due to surface tension and viscosity, analogous to the situation of dip coating. Table II gives a comparison of the values of U taken at this condition, U_i, with the correlation of Burley and Jolly[13] shown in (1). The table also lists data from the studies of Wilkinson[9] for roll coating and from the work of Blake *et al.*[4,12] for curtain coating onto dry substrates, for which values of $U_{\max}$ are also given. Table II shows that Eq. (1) gives a reasonable prediction of U_i for curtain coating onto dry substrates.

However, the correlation substantially underpredicts U_i for the data of Wilkinson[9] and the current work; the differences, typically of the order of 0.15–0.2 $\mathrm{ms^{-1}}$, are due to the presence of the prewet film. The discrepancies for the high viscosity liquids may not be surprising since Eq. (1) is only expected to hold for $0.2<\sigma/\mu<3.2$, and for $\mu \geqslant 365$ mPa s, the values are outside this range.

The values of the film thicknesses, c, in the current study are classified as "thick" according to Chen *et al.*[17] In their study, the deformation of the interface was dependent on whether the thickness was $O(10^{-10})$ m or $O(10^{-8}-10^{-6})$ m. Hence the exact value of the thickness of the film is not the main concern here, but the order of magnitude.

Although the thickness of the prewet film can be altered by adjusting the tension of the squeegee blades on the wheel cleaning system, regardless of the film thickness, higher values of U_i are obtained for coating onto a prewet surface than for coating onto dry ones. Table II also shows that no correlation can be found for $U_{\max}$ or U_i in terms of a critical Capillary number, despite this approach being used successfully by Lorenceau *et al.*[23] and Bolton and Middleman[32] for entrainment through cusp-like interfaces. This is not surprising given the profound inertial influence in curtain coating.

The data in Fig. 8(a) show a change in behavior at $\mu=0.462$ Pa s, and the established trend of decreasing values of $U_{\max}$ with increasing viscosity no longer applies. On increasing the viscosity further to 0.878 Pa s and at suitably high flow rates ($Q>3\ \mathrm{cm^2\ s^{-1}}$), substrate velocities clearly exceed all those obtained for lower viscosities. Unfortunately, due to the pumping limitations of the equipment used, data for $Q>4.85\ \mathrm{cm^2\ s^{-1}}$ and the upper branch of the curve could not be determined for the highest viscosity used (0.878 Pa s). At these viscosities, the thickness of the film is of $O(10^{-6})$ m and hence "macroscopic," but still in the same general classification as for lower viscosity fluids. This switch in behavior at high liquid viscosities has been noted before by Yamamura *et al.*[21] onto prewetted substrates, although no estimate of c was given, and by Clarke[11] and Benkreira,[8] both onto roughened substrates.

By increasing the curtain height to 95 mm, the data in Fig. 8(b) show that much higher maximum substrate veloci-

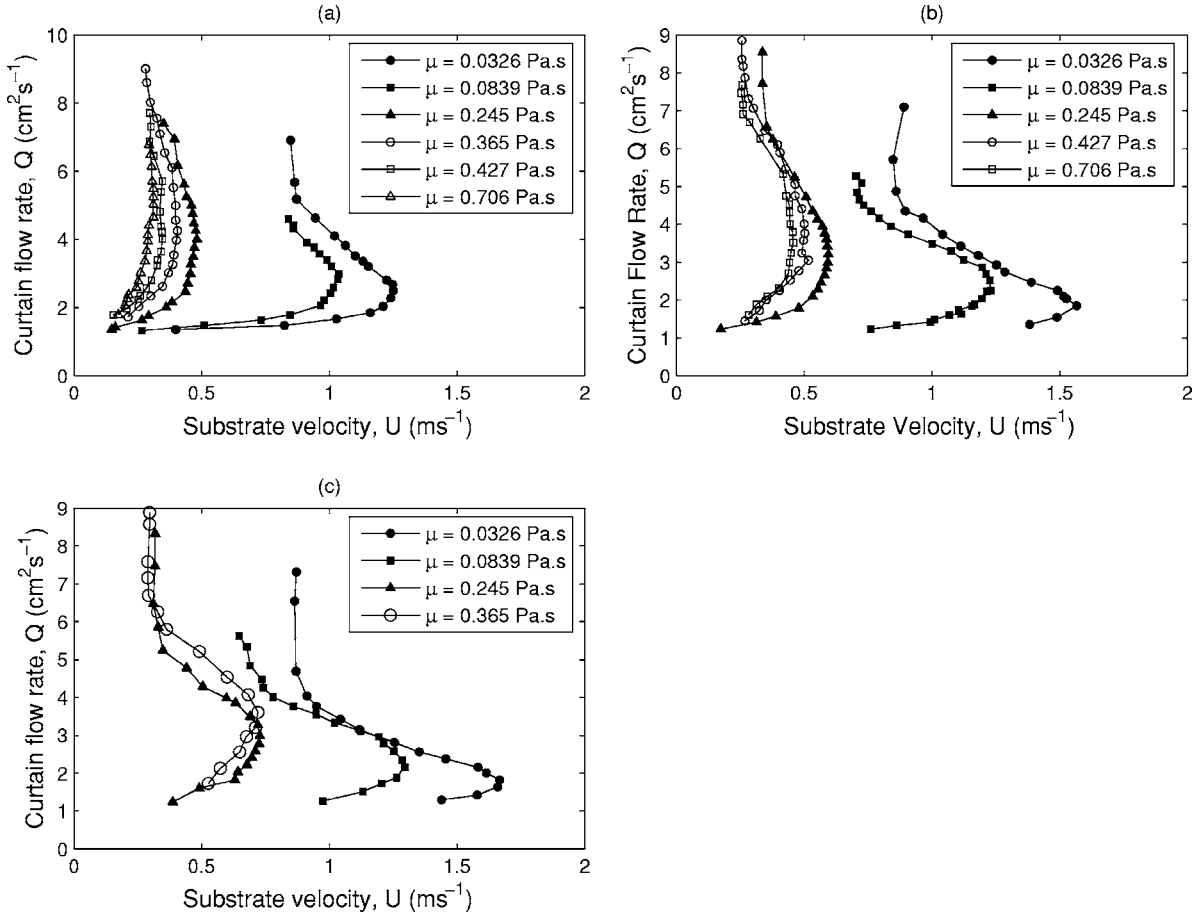

FIG. 7. Air entrainment curves for three set heights: (a) 35 mm, (b) 65 mm, and (c) 85 mm—low viscosity. The legends indicate viscosity in Pa s. $c=O(10^{-6})$ m.

ties can be achieved by use of a high viscosity fluid; this is similar to the intense hydrodynamic assist observed by Blake *et al.*[12] for coating onto dry substrates. The intense assist is manifested by a distinct change in the slope of the curve, which occurs at a flow rate of approximately 3 cm^2 s^{-1}, and vast increases in substrate velocity for small increases in curtain flow rate are experienced until a threshold flow rate is exceeded where the velocities drop dramatically. This can be seen for all the fluids used to produce Fig. 8(b) with $\mu \geqslant 0.462$ Pa s.

Figure 9 plots $U_{\max}$ from Figs. 7 and 8 versus μ. The values of $U_{\max}$ have been normalized by the impingement

TABLE II. Comparison of air entrainment data for selected curtain heights and viscosities. Dry web and prewet refer to the substrate. $U_{\max}$ corresponds to the maximum substrate velocity, U_i the velocity that is independent of flow rate, and the numbers in brackets are the corresponding Capillary numbers. The final column is the velocity predicted by Burley and Jolly (1984) for dip coating.

Data	μ (Pa s)	Coating method	$U_{\max}$ (ms^{-1}), (Ca$_m$)	U_i (ms^{-1}), (Ca$_i$)	U_{bj} (ms^{-1})
Blake '99	0.025	3 cm curtain, dry web	0.8 (0.31)	0.7 (0.27)	0.81
Blake '99	0.057	3 cm curtain, dry web	0.47 (0.42)	0.4 (0.36)	0.43
Blake '04	0.320	10.2 cm curtain, dry web	0.21 (1.03)	0.12 (0.59)	0.115
Wilkinson	0.245	immersed roll	n/a	0.39 (1.33)	0.14
Fig. 7	0.0326	3.5 cm curtain, prewet	1.25 (0.60)	0.84 (0.40)	0.69
Fig. 9	0.0326	8.5 cm curtain, prewet	1.66 (0.79)	0.86 (0.41)	0.69
Fig. 7	0.245	3.5 cm curtain, prewet	0.48 (1.79)	0.35 (1.31)	0.14
Fig. 11	0.365	9.5 cm curtain, prewet	0.85 (4.77)	0.29 (1.63)	0.10
Fig. 10	0.427	8.5 cm curtain, prewet	0.583 (3.85)	0.25 (1.65)	0.09
Fig. 11	0.462	9.5 cm curtain, prewet	1.81 (12.86)	0.25 (1.77)	0.087
Fig. 11	0.552	9.5 cm curtain, prewet	2.256 (19.22)	0.22 (1.87)	0.075
Fig. 10	0.706	8.5 cm curtain, prewet	0.64 (6.98)	0.25 (2.73)	0.06

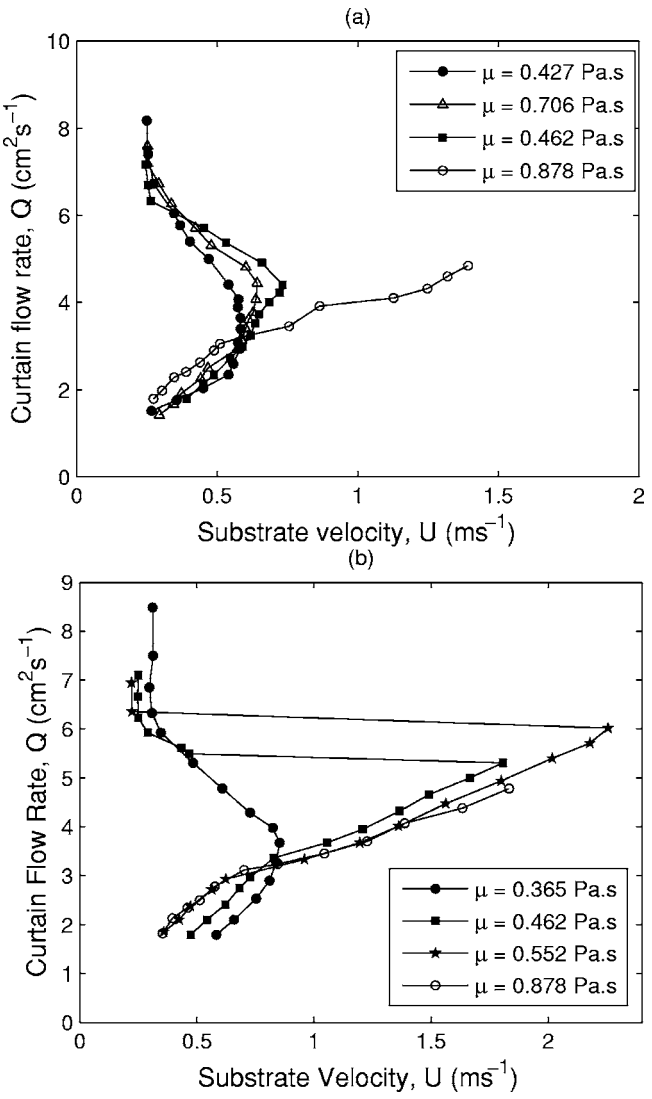

FIG. 8. Air entrainment curves for (a) 85 mm—high viscosity and (b) 95 mm. The legends indicate viscosity in Pa s. $c=O(10^{-6})$ m.

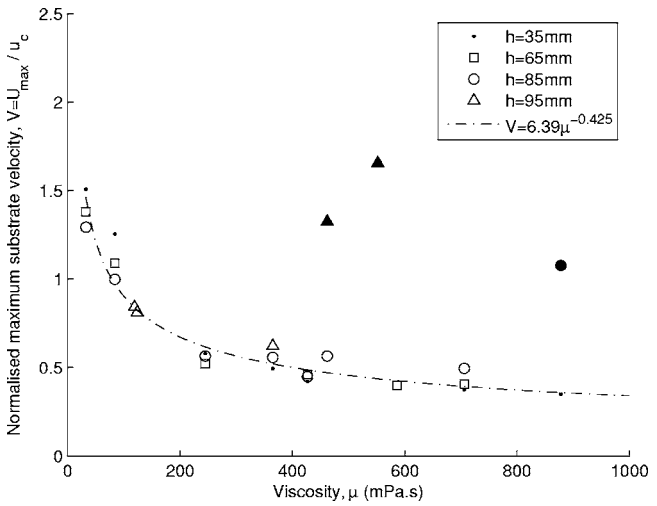

FIG. 9. Plot of maximum substrate velocity (normalized by the impingement velocity) versus viscosity for all curtain heights. The dot-dash line is the equation $V=6.39\ \mu^{-0.425}$. Filled symbols indicate data taken from "intense assist" experiments.

speed $u_c=\sqrt{2gh}$, a similar approach to Clarke.[11] By excluding the data points obtained for the high viscosity and impingement speed regime, a fit to the data is achieved, shown by the dashed curve. This correlation is given by $V=U_{\max}/u_c=6.39\mu^{-0.425}$ with $R^2=0.94$. This correlation is not valid throughout the high viscosity-impingement speed regime, as can be seen from the data points. As yet, violation of this inverse relationship between $U_{\max}$ and μ has only been observed in this regime for the prewet surface and is yet to be reported for smooth dry substrates by increasing the viscosity alone, although the intense assist reported by Blake *et al.*[12] for much greater curtain heights is qualitatively similar.

Figure 10(a) demonstrates the effect of increasing the film thickness upon the air entrainment velocity of a low viscosity fluid (0.124 Pa s) at a constant curtain height of 95 mm. Three distinct curves are produced for three different film thicknesses. The maximum substrate velocity increases for increasing c and there is a marked increase in U_i. An opposite effect is noted for a higher viscosity fluid in Fig. 10(b) for a 0.462 Pa s solution at a curtain height of 95 mm. In this case, when the carrier layer is of the order of 10^{-6} m, intense hydrodynamic assist is observed giving a maximum substrate velocity of 1.81 ms^{-1}, which is lost on increasing the thickness of the layer to the order of 10^{-5} m producing a maximum substrate velocity of 0.83 ms^{-1}. The two curves coincide almost exactly for low flow rates and also tend to the same limiting value of U_i. The values for $U_{\max}$ and U_i for Figs. 10(a) and 10(b) are tabulated in Table III. This observation, along with that of intense assist for high viscosity, is, as yet, unexplained.

Blake *et al.*[3] showed that it was possible to produce a "master" air entrainment curve for fluids of viscosities ranging from 0.063–0.22 Pa s by plotting the normalized relative wetting line position (which gives a measure of the location of the wetting line with respect to the rear surface of the curtain) versus normalized substrate velocity (at the clearing of air entrainment). A similar set of air entrainment curves may be produced by plotting a modified Reynolds number at the onset of air entrainment, $\mathrm{Re}_m=\rho Q u_c/\mu U_{ae}$, versus normalized substrate velocity ($U'=U/U_{\max}$), although these are not shown here.

Using a Sakiadis-type boundary layer, Blake *et al.*[3] developed a theoretical prediction for the relative wetting line position (rwlp) as a function of substrate velocity for given flow conditions. Using similar analysis, the following equation for the prediction of the rwlp can be deduced:

$$l=\frac{L_b}{w}=\frac{9}{20}\left(1-\frac{10\sigma}{3\rho Q u_c}\right)\frac{\rho Q u_c}{\mu U}, \tag{2}$$

where L_b is the length of the boundary layer, which extends from the contact line to the front surface of the curtain (see Blake *et al.*[3] for more details).

Experimentally, we determine the rwlp by measuring the distance from the point of contact of the liquid curtain with the prewet film to the rear surface of the curtain. An example

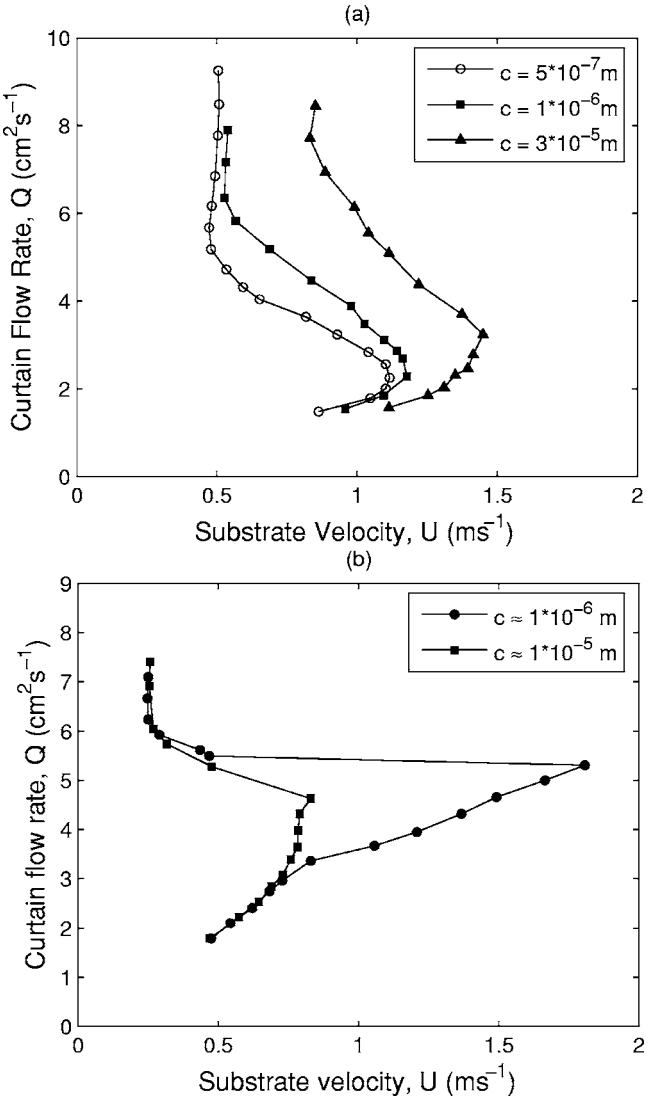

FIG. 10. Air entrainment curves for increasing carrier layer thickness for (a) 0.124 Pa s and (b) 0.462 Pa s.

of this is given in Fig. 11 for a 0.075 Pa s solution. This measurement is performed for a series of still images. Then we calculate the rwlp by the following:

$$l = \frac{L_b}{w} = \frac{x+w}{w} = 1 + \frac{xu_c}{Q}, \tag{3}$$

where $x = L_b - w$ is the measurement taken from the images and can take positive or negative values.

Figures 12(a) and 12(b) plot experimental data against the prediction (2) for a number of flow conditions. The choice of liquids ($\mu = 0.075, 0.172$ Pa s) and curtain height ($h = 60$ mm) here were essentially arbitrary, but show all the qualitative features. Figure 12(a) for the lower viscosity fluid shows reasonable agreement with the model over three selected flow rates. For the two higher flow rates, the high values of l correspond physically to the contact line located to the rear of the curtain, i.e., a "heel" formation, and Eq. (2) provides a reasonable fit throughout the range of speeds tested. For the lowest flow rate, the final data point at $U = 1.24$ ms^{-1}, $l = 0.26$ is much lower than might be expected

TABLE III. Maximum and flow field independence substrate velocities for increasing film thicknesses corresponding to data from Figs. 10(a) and 10(b).

Viscosity (Pa s)	Film thickness (m)	U_{max} (ms^{-1})	U_i (ms^{-1})
0.124	5×10^{-7}	1.11	0.503
0.124	1×10^{-6}	1.17	0.526
0.124	3×10^{-5}	1.45	0.832
0.462	1×10^{-6}	1.807	0.247
0.462	1×10^{-5}	0.829	0.254

given that the predicted "optimum" value of $l' = 0.7$,[33] after which air entrainment is expected (it should be noted, however, that this predicted optimum value only applies to U_{max}). In Fig. 12(b), the fit to experimental data is poorer. At the lowest speeds for the two higher flow rates, the model significantly underpredicts l, although for $U > 0.5$ ms^{-1}, a better fit is obtained. The sharp increase in l for the final data point for $Q = 3.21$ cm^2 s^{-1} corresponds to air entrainment. For the lowest flow rate in Fig. 12(b), the model clearly underestimates l. In both Figs. 12(a) and 12(b), the horizontal line represents $l = 0.7$ and the vertical lines represent U_{max}. The flow rates at which U_{max} was obtained were $Q = 2.2$ and 2.6 cm^2 s^{-1} and the predicted values of the rwlp are 0.32 and 0.39, respectively [note that this was not measured experimentally, but calculated using Eq. (2)]. These values are much lower than the predicted value of 0.7.

The discrepancies in the data and the model and the low values of l obtained may be understood by considering the residual film on the wheel surface, which is likely to alter the viscous drag experienced by the impinging curtain and the adhesion between the curtain and the residual film.

This analysis is used to illustrate the fact that although the surface is known to be prewet, treatment of the surface as "dry" can lead to quantitative agreement between experimental data and theoretical predictions. This naturally leads to the question of whether a thin viscous film, though many

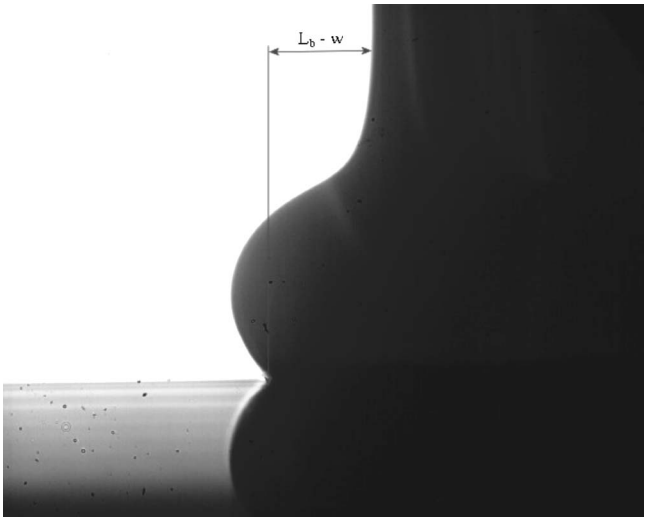

FIG. 11. Image showing the measurement of the position of the contact line relative to the rear of the curtain ($L_b - w$). The flow rate $Q = 2.71$ cm^2 s^{-1} and the substrate speed $U = 0.41$ ms^{-1}. $h = 60$ mm.

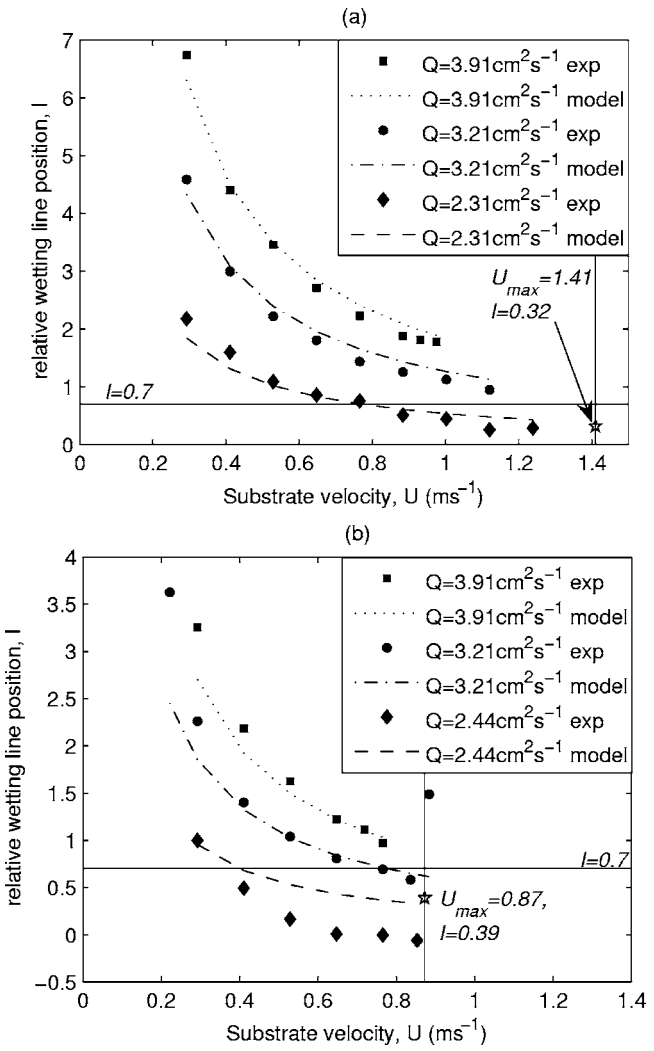

FIG. 12. Relative wetting line position plotted as a function of substrate velocity for (a) 0.075 Pa s and (b) 0.172 Pa s solutions. The plots show both experimental data points and curves generated from Eq. (2). The sharp increase in (b) for $Q=2.44$ cm^2 s^{-1} corresponds to air entrainment. The vertical lines correspond to $U_{\max}$ and the data point on these lines plots the value of l at the corresponding conditions. $h=60$ mm.

molecular layers thick, can act like a dry support in terms of the wetting mechanism. This is likely to be important for mathematical modeling of such flows. In light of this, the concept of flow-rate-dependent contact angles[4,34] needs to be readdressed since, although quantitatively the results are different from a dry tape, the qualitative features of true dynamic wetting in curtain coating (including flow-rate-dependent air entrainment velocities) are observed when there may not even be a contact angle present. Also, the microscopic physics of forcing a liquid to contact a preexisting liquid film may have similarities to the process of forcing a liquid onto a dry surface, which may be important to further our understanding of dynamic wetting.

IV. CONCLUSIONS

An experimental study of the hydrodynamic influence in curtain coating onto a prewetted surface of varying film thicknesses has been performed for a range of fluid properties, substrate velocities, curtain flow rates, and curtain heights.

The mechanism of hydrodynamic assist is confirmed for a curtain impinging onto a prewet surface and successful coating was achieved up to Capillary numbers of $O(20)$. The amount of assist can be altered by changing the fluid viscosity and, in certain cases, violates the established inverse viscosity dependence. This has yet to be reported for dry substrates.

The role of the film prewetting the substrate was also studied, and results indicate that the influence of the thickness of the residual film is qualitatively different for different parameter regimes—increasing the thickness led to higher maximum substrate velocities for a low viscosity fluid, but decreased the maximum substrate velocity for a high viscosity fluid when intense assist is observed.

Treatment of the surface as a dry substrate can lead to agreement between experimental data and theoretical predictions in terms of the relative wetting line position, further demonstrating the similarities between a viscous liquid film and a solid dry surface in terms of wetting.

The physics of the mechanism of air entrainment in coating onto a prewet surface may be considered as analogous to that in cusp-like interfaces; while also being subjected to the same hydrodynamic influences that would be observed in the coating of dry substrates. The results presented in this paper illustrate that the nonlocal dependence of coating flows is not restricted to dynamic wetting problems, and that *hydrodynamic assist* is a generic phenomenon of free-surface flows.

[1] E. B. Dussan V., "On the spreading of liquids on solid surfaces: Static and dynamic contact lines," Annu. Rev. Fluid Mech. **11**, 371 (1979).
[2] T. D. Blake, "The physics of moving wetting lines," J. Colloid Interface Sci. **299**, 1 (2006).
[3] T. D. Blake, A. Clarke, and K. J. Ruschak, "Hydrodynamic assist of dynamic wetting," AIChE J. **40**, 229 (1994).
[4] T. D. Blake, M. Bracke, and Y. D. Shikhmurzaev, "Experimental evidence of nonlocal hydrodynamic influence on the dynamic contact angle," Phys. Fluids **11**, 1995 (1999).
[5] Š. Šikalo, C. Tropea, and E. N. Ganić, "Dynamic wetting angle of a spreading drop," Exp. Therm. Fluid Sci. **29**, 795 (2005).
[6] R. Burley and S. B. Kennedy, "An experimental study of air entrainment at a solid/liquid/gas interface," Chem. Eng. Sci. **31**, 901 (1976).
[7] T. D. Blake and Y. D. Shikhmurzaev, "Dynamic wetting by liquids of different viscosity," J. Colloid Interface Sci. **253**, 196 (2002).
[8] H. Benkreira, "The effect of substrate roughness on air entrainment in dip coating," Chem. Eng. Sci. **59**, 2745 (2004).
[9] W. L. Wilkinson, "Entrainment of air by a solid surface entering a liquid/air interface," Chem. Eng. Sci. **30**, 1227 (1975).
[10] H. Benkreira, "Experimental study of dynamic wetting in reverse-roll coating," AIChE J. **48**, 221 (2002).
[11] A. Clarke, "Coating on a rough surface," AIChE J. **48**, 2149 (2002).
[12] T. D. Blake, R. A. Dobson, and K. J. Ruschak, "Wetting at high capillary numbers," J. Colloid Interface Sci. **279**, 198 (2004).
[13] R. Burley and R. P. S. Jolly, "Entrainment of air into liquids by a high speed continuous solid surface," Chem. Eng. Sci. **39**, 1357 (1984).
[14] O. Cohu and H. Benkreira, "Angling the wetting line retards air entrainment in premetered coating flows," AIChE J. **44**, 1207 (1998).
[15] R. A. Buonopane, E. B. Gutoff, and M. M. T. Rimore, "Effect of plunging tape surface properties on air entrainment velocities," AIChE J. **32**, 682 (1986).
[16] T. D. Blake, A. Clarke, and E. H. Stattersfield, "An investigation of electrostatic assist in dynamic wetting," Langmuir **16**, 2928 (2000).
[17] X. Chen, E. Rame, and S. Garoff, "The effects of thin and ultrathin liquid films on dynamic wetting," Phys. Fluids **16**, 287 (2004).

[18]T. R. O'Connor, "Coating apparatus provided with a protective shield," U.S. Patent 4,287,240, 1981.
[19]D. A. Dittman and A. Rozzi, "Method of multi-layer coating," U.S. Patent 4,001,024, 1977.
[20]M. S. Bermel, S. P. McKeown, and K. J. Ruschak, "Slide bead coating with a low viscosity carrier layer," U.S. Patent 6,579,569, 2003.
[21]M. Yamamura, S. Suematsu, K. Toshihisa, and K. Adachi, "Experimental investigation of air entrainment in a vertical liquid jet flowing down onto a rotating roll," Chem. Eng. Sci. **55**, 931 (1999).
[22]D. D. Joseph, J. Nelson, M. Renardy, and Y. Renardy, "Two-dimensional cusped interfaces," J. Fluid Mech. **223**, 383 (1991).
[23]E. Lorenceau, F. Restagno, and D. Quere, "Fracture of a viscous liquid," Phys. Rev. Lett. **90**, 018450 (2003).
[24]J. Eggers, "Air entrainment through free-surface cusps," Phys. Rev. Lett. **90**, 184501 (2003).
[25]D. D. Joseph, "Understanding cusped interfaces," J. Non-Newtonian Fluid Mech. **44**, 127 (1992).
[26]J. Jeong and H. K. Moffatt, "Free-surface cusps associated with flow at low Reynolds number," J. Fluid Mech. **241**, 1 (1992).
[27]Y. D. Shikhmurzaev, "On cusped interfaces," J. Fluid Mech. **359**, 313 (1998).
[28]Y. D. Shikhmurzaev, "Singularity of free-surface curvature in convergent flow: Cusp or corner?" Phys. Lett. A **345**, 378 (2005).
[29]O. Cohu and H. Benkreira, "Entrainment of air by a solid surface plunging into a non-Newtonian liquid," AIChE J. **44**, 2360 (1998).
[30]J. O. Marston, S. P. Decent, and M. J. H. Simmons, "Hysteresis and non-uniqueness in the speed of the onset of instability in curtain coating," J. Fluid Mech. **569**, 349 (2006).
[31]C. L. Bower, "Method for avoiding recirculation effects in curtain coating," U.S. Patent 6,472,021, 2002.
[32]B. Bolton and S. Middleman, "Air entrainment in a roll coating system," Chem. Eng. Sci. **35**, 597 (1980).
[33]S. J. Weinstein and K. J. Ruschak, "Coating flows," Annu. Rev. Fluid Mech. **36**, 29 (2004).
[34]M. C. T. Wilson, J. L. Summers, Y. D. Shikhmurzaev, A. Clarke, and T. D. Blake, "Nonlocal hydrodynamic influence on the dynamic contact angle: Slip models versus experiment," Phys. Rev. E **73**, 041606 (2006).